Vibrational dynamics and Raman scattering in fractals: A numerical study

V.Mazzacurati
Dipartimento di Fisica, Università di Roma "La Sapienza," Piazza Aldo Moro 2, Roma, I-00185, Italy

M.Montagna
Dipartimento di Fisica, Università di Trieste, Via Valerio 5, Trieste, I-34127, Italy

O.Pilla and G.Viliani
Dipartimento di Fisica, Università di Trento, Povo, Trento, I-38050, Italy

G.Ruocco and G.Signorelli
Dipartimento di Fisica, Università di L'Aquila, Via Vetoio, Coppito, L'Aquila, I-67100, Italy
(Received 10 June 1991)

The vibrational dynamics and Raman coupling coefficient of site percolating structures have been studied numerically. The main results that emerge from this work are the following: (i) Characterization of fractons in k space clarifies the oscillatory nature of the modes and allows an average wavelength to be defined, which is more correlated with frequency than the localization length, which fluctuates strongly; (ii) in these systems, it is not easy to define a local strain due to their essentially disordered structure; (iii) the Raman coupling coefficient $C(\omega)$ was calculated in the dipole-induced-dipole and bond-polarizability approximations. The scaling laws proposed so far for $C(\omega)$ do not reproduce the results of our simulation; the difficulty of finding a scaling law in terms of the fractal macroscopic parameters is discussed.

I. INTRODUCTION

The dynamical and static properties of deterministic and random fractals have been a subject of extensive investigation. One reason for such interest is that the dynamics of fractals is expected to share some characteristics with that of real disordered systems,[1] which, however, are exceedingly difficult to handle.

In particular, for real systems it is interesting to know both the density of vibrational states and the shape and extension of the localized vibrational wave functions, which determine thermal and transport properties.

Low-frequency anelastic light scattering is a powerful tool for obtaining information on the vibrational dynamics. Since the time when the observation of Raman scattering from (presumably) fractal structures was reported in aerogels,[2] metallic clusters,[3] and glasses,[4] systematic experimental investigation has been carried out on silica aerogels.[5–11]

The observed power-law dependence on frequency of the reduced spectrum in the acoustic low-frequency region was explained on the basis of models exploiting the scaling properties of the local strain. In this way, the observed exponent was related to the parameters, which describe the static and dynamic scale invariance of fractals.

Different expressions for the Raman coupling coefficient were derived; this induced us to test the proposed models by performing a numerical simulation on model systems consisting of square and cubic site-percolation clusters with equal masses and force constants. We computed the Raman coupling coefficient in the dipole-induced-dipole (DID) and bond-polarizability (BP) frameworks by assuming spherical polarizable units in each occupied site of the cluster. A brief report of our results was published in a recent paper;[12] in the present paper we report more extensive data and discuss them.

In Sec. II we describe briefly the numerical procedure and the relative checks; in Sec. III we discuss the characteristic features of the vibrational eigenmodes; the properties of the dynamical structure factor are discussed in Sec. IV, while the formalism for the Raman coupling coefficient is developed in Sec. V; our numerical results are presented in Sec. VI and discussed in Sec. VII.

II. NUMERICAL METHOD

The systems we considered were square and cubic site percolation clusters containing N identical masses ($M = 1$) and with identical force constants ($K = 1$) between nearest neighbors.[13–17] The frequency and eigenvectors of the normal modes of the system ("fractons") are provided by diagonalization of the dynamical matrix; indeed the displacement of the ith mass from its equilibrium position $\mathbf{r}^i$ can be written as

$$\mathbf{u}^i(t) = \sqrt{\frac{\hbar}{2MN}} \sum_p \frac{1}{\sqrt{\omega_p}} \mathbf{e}(i|p) A_p(t), \tag{1}$$

where p is the fracton index, $p = 1, 2, \ldots, Nd$ (where d

is the space dimensionality), ω_p its frequency, and $\mathbf{e}(i|p)$ are real and orthonormal vectors, which (apart from the solution at $\omega = 0$) do not shift the center of mass, i.e.,

$$\sum_i \mathbf{e}(i|p) \cdot \mathbf{e}(i|p') = \delta_{pp'},$$
$$\sum_i \mathbf{e}(i|p) = 0. \tag{2}$$

The corresponding quantities in the case of phonons would be $(p \rightarrow \mathbf{k}, \chi)$

$$\mathbf{e}(i|p) \equiv \mathbf{e}(i|\mathbf{k},\chi) = \frac{1}{\sqrt{N}} \hat{\boldsymbol{\epsilon}}(\mathbf{k},\chi) e^{i\mathbf{k}\cdot\mathbf{r}^i} \tag{3}$$

where $\hat{\boldsymbol{\epsilon}}(\mathbf{k},\chi)$ is the polarization vector.

We assumed scalar elasticity, which reduced the matrix to be diagonalized to an $N \times N$ one because in this case each eigenvalue is d-fold degenerate. In this case the polarizations of the normal modes of the system are always parallel to the axis of the square (or cubic) lattice, and the quantity $\mathbf{e}(i|p)$ can be treated as a scalar. We also imposed cyclic boundary conditions.

The maximum number of masses that could be handled by a Cray Research, Inc. YMP computer was of the order of 4300, around which value the EISPACK diagonalization routine started to fail, especially for the low-energy eigenvectors. A series of preliminary checks was performed to test the reliability of the results.

(i) The baricenter of the system should be conserved by each mode.

(ii) The Raman scattering of a perfect lattice should be zero.

(iii) The nearest-neighbor potential energy should vary as ω^2.

In all cases the departure from these conditions was small enough to ensure that the eigenfunctions were sufficiently accurate up to matrix dimensions of about 4000x4000.

III. CHARACTERIZATION OF FRACTONS

As is known, the disordered nature of fractals tends to localize the eigenvectors in a finite volume; it was suggested[18,19] that the modes could be characterized by a single energy-dependent parameter, i.e., the localization length l, which in turn defines the localization volume l^D, where D is the fractal dimension. From scaling arguments[18,19] it was found that any such parameter, to be relevant, should obey the dispersion relation

$$l \propto \omega^{-\bar{d}/D}, \tag{4}$$

where $\bar{d}$ is the spectral dimension.[18] Equation (4) was thought to be the fracton analogue of the long-wavelength acoustic phonon relation

$$\lambda \propto \omega^{-1}.$$

The localized nature of fractons, as opposed to the propagating one of phonons, was represented[1] by the following superexponentially decaying wave function:

$$|e(i|p)|^2 \propto l_p^{-D} e^{-[|\mathbf{r}^i - \mathbf{r}_p|/l_p]^{d_\phi}}, \tag{5}$$

where $\mathbf{r}_p$ is the coordinate of the fracton center of mass, l_p is the localization length of mode p, and d_ϕ is the superlocalization exponent. High d_ϕ values give rise to steplike functions of width l_p. By averaging over many neighboring modes of two-dimensional percolation clusters and by fitting the mean fracton shape to Eq. (5), the dispersion relation (4) was verified and the value $d_\phi = 2.3$ was derived.[17] Equation (5) has the obvious disadvantage of neglecting spatial oscillations, which are required by Eq. (2). As we shall see in the following, Eq. (5) may at most represent squared modes averaged on a certain frequency range, and the look of individual actual fractons bears no resemblance to it. Even worse, the square root of (5) has been used as wave function[2,3,20] in the calculation of scattering properties.

The difficulty of characterizing fractons by an analytical function like (5) is evident when looking at Figs. 1(a) and 1(b), where two eigenvectors relative to two adjacent modes of a 65×65 square percolation cluster, of energies 0.802 04 (mode A) and 0.803 44 (mode B) respectively, are depicted. It is obvious that the two nearly degenerate modes have very different localization lengths. However, the distances among groups of masses, which move with the same phase, appear to be on average the same. This is more evident in Figs. 1(c) and 1(d), where the same fractons are shown in a logarithmic scale in order to evidence small, otherwise hidden displacements of masses in the most localized mode. Although we did not attempt any quantitative analysis of the average spatial oscillation periods, visual inspection confirms that these periods are very similar. Therefore, it is not the localization length, but rather the *wavelength* of the disordered, spatial oscillations that is important in determining the energy: We expect that the Fourier transforms of these modes are much more similar to each other than are the modes themselves.

We have therefore analyzed the normal modes in the reciprocal space, by defining the (normalized) transform as

$$f(\mathbf{k},p) = \frac{1}{m} \sum_i e^{i\mathbf{k}\cdot\mathbf{r}^i} e(i|p), \tag{6}$$

where m is the linear dimension of the cyclic lattice on whose sites the fractal cluster is defined (here $m = 65$). The squared moduli of $f(\mathbf{k},p)$ are reported in Figs. 3(a) and 3(b) (three-dimensional plots) and 3(c) and 3(d) (contour maps) in the $k_x - k_y$ space for the same fractons as in Figs. 1(a) and 1(b).

Very broad wave packets are observed: The more localized nature of mode B is reflected in its smoother transform. However, these wave packets corresponding to nearly degenerate fractons have a maximum at very close values of $|\mathbf{k}|$. In order to better quantify this concept let us define the function $\mathcal{F}(k,p)$

$$\mathcal{F}(k,p) = \frac{1}{2\pi k} \int d\mathbf{k} |f(\mathbf{k},p)|^2 \delta(k - |\mathbf{k}|), \tag{7}$$

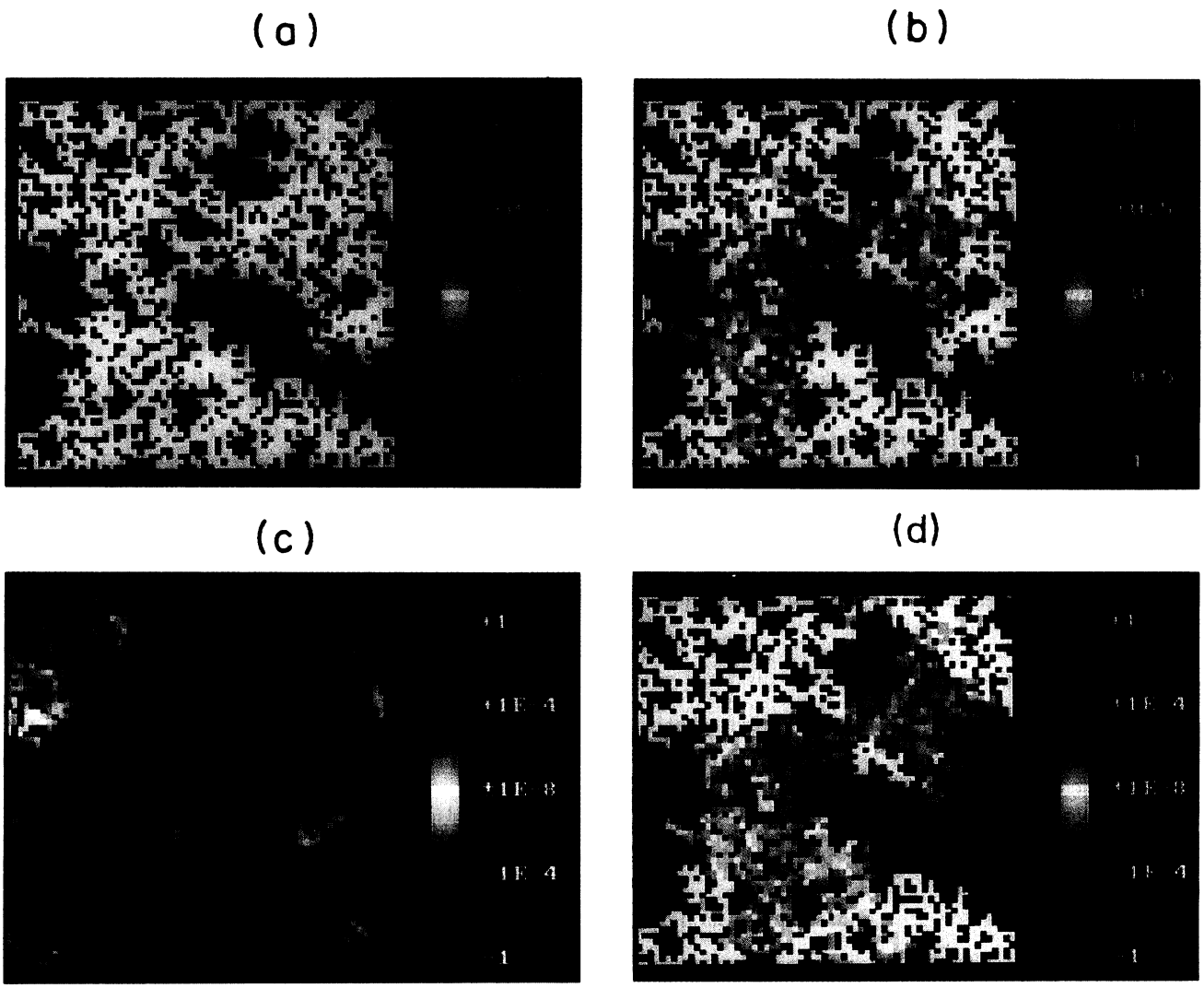

FIG. 1. Vibrational amplitudes of two successive fractons of a 65×65 cluster at percolation threshold. (a) $\omega_1 = 0.802\,04$ (mode A); (b) $\omega_2 = 0.803\,44$ (mode B). (c) and (d), same as (a) and (b) but in a logarithmic scale to enhance the oscillatory behavior of the fracton tails. Frequency in $\sqrt{K/M}$ units: Debye frequency is $2\sqrt{2}$.

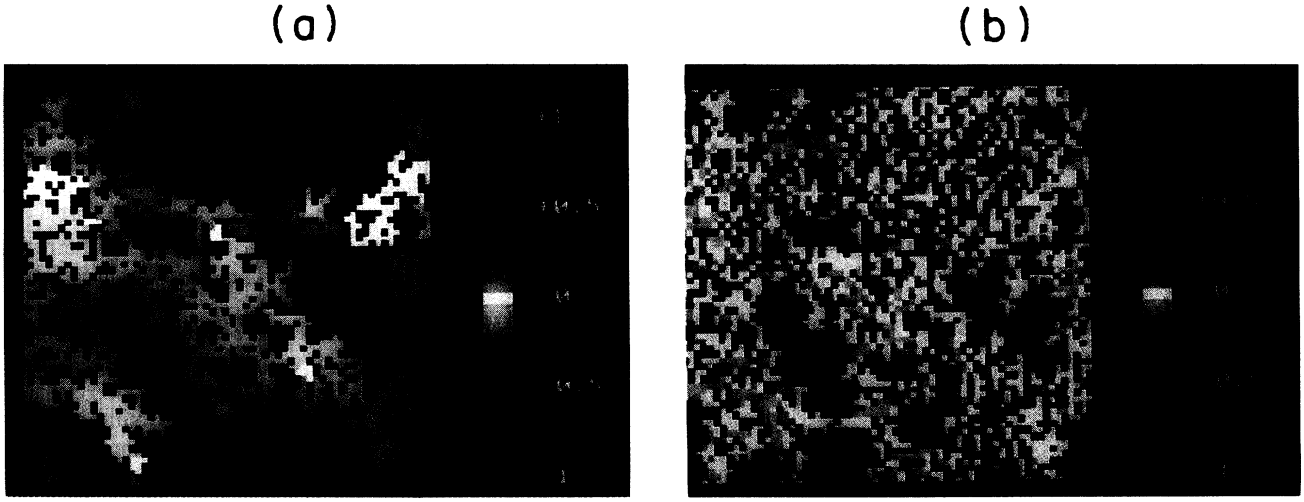

FIG. 2. (a) Vibrational amplitudes of a low-frequency mode ($\omega = 0.022$) of a 65×65 cluster at percolation threshold ($c = 0.59$). (b) displacement difference of any pair of neighboring masses in the x direction (see text).

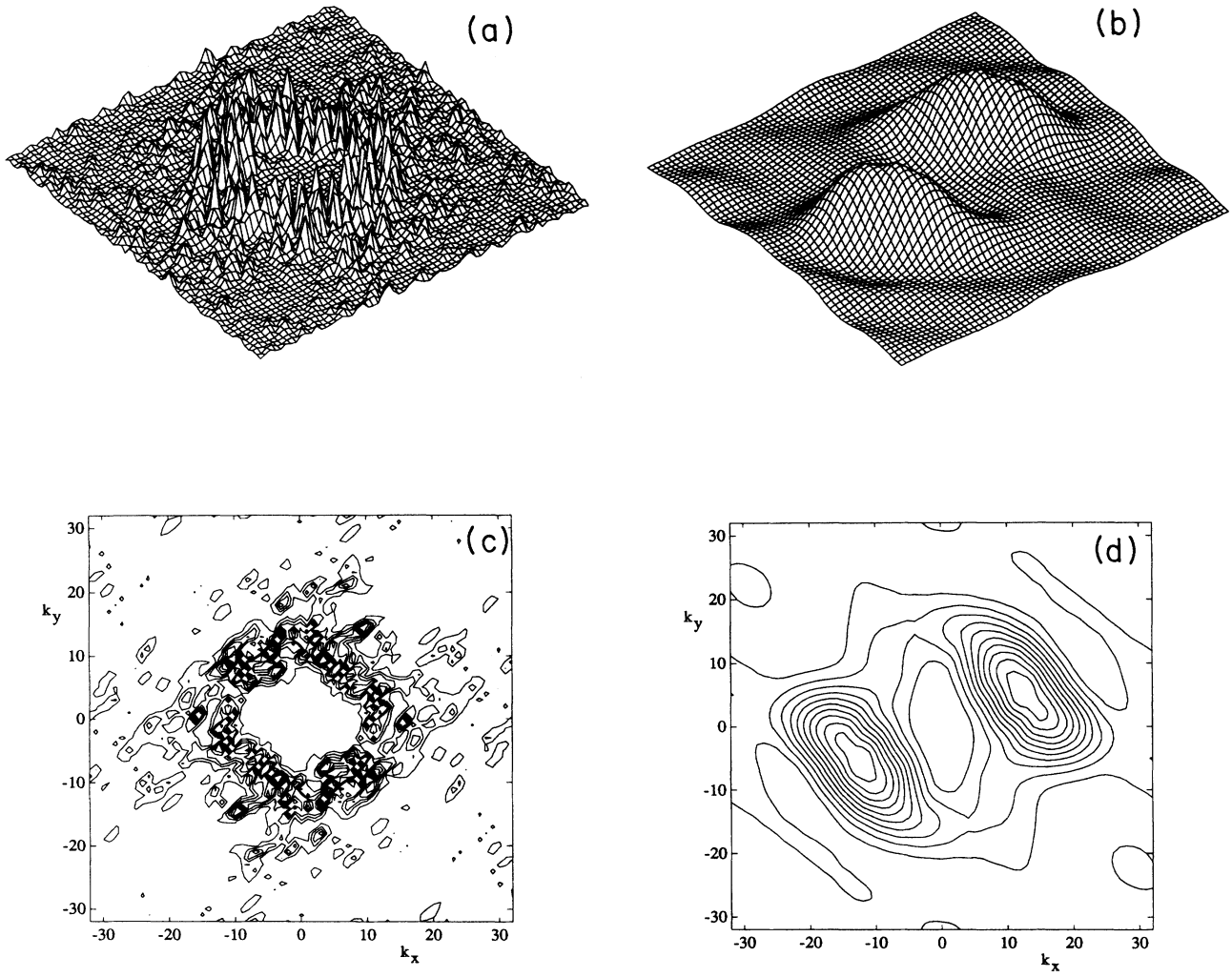

FIG. 3. Squared Fourier transforms in the (k_x, k_y) space of the two fractons shown in Fig. 1. (a) and (c), mode A; (b) and (d), mode B. The k values are in units of $2\pi/L$, where $L = 65a$ is the lattice size.

which is an average over all directions in the k_x-k_y plane of the dynamical structure factor of mode p. This function has large fluctuations, but after smoothing it is possible to determine the position of the maximum, $\mathcal{K}_p$, for each mode p. This analysis was performed for all modes of a two-dimensional cluster of concentration $c = 0.59$ (Fig. 4). As can be seen, at percolation $\mathcal{K}_p$ scales with frequency as $\mathcal{K}_p \propto \omega_p^{0.7} = \omega_p^{\bar{d}/D}$ over a wide range of frequencies; no average over different fractons was performed, contrary to what is required for the characterization of fractons in real space.[17] We also tried different ways of defining a characteristic $\mathcal{K}_p$ value for the wave packets, for example by taking the square root of the second moment of $\mathcal{F}(k,p)$; however, the values obtained in this way follow the scaling relation in a limited k range, which excludes the extremal values where the broad wave packets are asymmetric.

The same detailed analysis was performed for a concentration $c = 0.75$, for which a crossover from fractons to phonons is expected and actually observed at $\omega_{co} \approx 0.3$. For $\omega > \omega_{co}$ no significant changes are observed in the $\mathcal{K}_p$ vs ω_p relation with respect to the cluster at the percolation threshold, while at lower frequencies a phononlike behavior ($\mathcal{K}_p \propto \omega_p$) is observed.

True phonons in an ordered system would produce eight peaks in the transform due to the eightfold degeneracy of the modes (the degeneracy is reduced to four when $|k_x| = |k_y|$ or when k_x or $k_y = 0$). A moderate disorder mixes these states, which are no longer degenerate, and induces only a slight mixing of other k values; when the disorder is increased the mixing also increases and broadens the wave packet, which retains a somewhat ringlike shape similar to, though less disturbed than, Fig. 3(a).

From this analysis it appears that also in the case

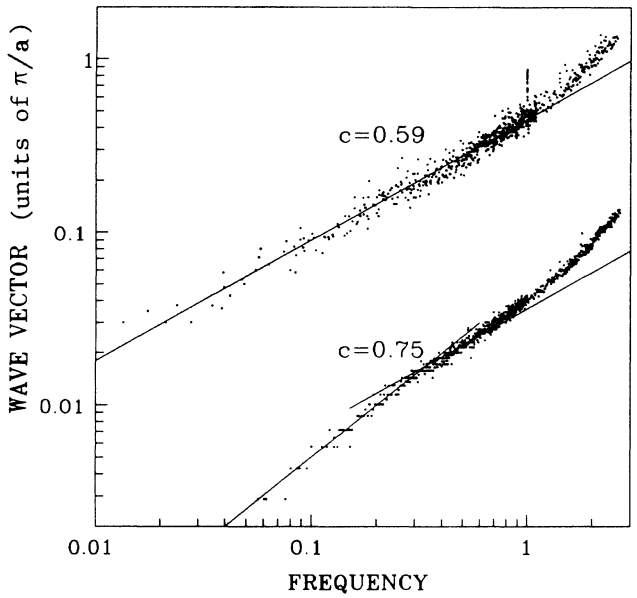

FIG. 4. $\mathcal{K}_p$ as a function of frequency, for two 65×65 lattices of different concentration, $c = 0.59$ and $c = 0.75$. For graphical reasons the points relative to c=0.75 are shifted downward by a decade, and for $\omega > 1$ only one point out of ten is plotted. The straight lines of slopes 0.704 ($= \bar{d}/D$) and 1 are reported as guides to the eye.

of fractons is possible to define a sort of wavelength, $\lambda_p = 2\pi/\mathcal{K}_p$, which determines the vibrational frequency according to the dispersion relation $\lambda_p \propto \omega_p^{-\bar{d}/D}$. As mentioned, the localization length of individual fractons, whichever its definition, is a greatly fluctuating function of ω, and only its average value over many fractons obeys the same dispersion relation.

The question now arises whether there exists any scaling argument for evaluating matrix elements involving fracton wave functions. In general, the concept of local strain has been widely used for approaching this problem; for phonons the local strain behaves as $k \propto \omega$, and for fractons the assumption has been made that it behaves as $l_p^{-d_\phi} \propto \omega_p^{\bar{d}d_\phi/D}$ (Ref. 2) [or $\omega_p^{\bar{d}\sigma/D}$ (Ref. 21)]. In view of the preceding discussion, it would seem more appropriate to use $\mathcal{K}_p \propto \omega_p^{\bar{d}/D}$; however, in our opinion the very concept of local strain loses most of its usefulness. In order to visualize the situation, let us consider a low-frequency mode on a percolating cluster such as in Fig. 2(a); the mode looks rather smooth. In Fig. 2(b) we report the eigenvector difference of any pair of masses, which are neighbors along a given direction, $e(i|p) - e(i+1|p)$. In any local strain formulation the eigenvectors $e(i|p)$ are considered as a continous spatial function, $e(i|p) \to e(\mathbf{r}^i|p)$, and the difference $e(i|p) - e(i+1|p)$ becomes equal to $ad[e(\mathbf{r}^i|p)]/dr \propto a\epsilon_{xx}(\mathbf{r}^i|p)$. Here a is the intermass distance and $\epsilon_{\alpha\beta}(\mathbf{r}|p)$ the tensorial strain field associated with mode p. As it is clearly seen, this quantity is not smooth: Its fluctuations are of the same order of magnitude as the quantity itself.

That fluctuations are essential is evident if we consider two limiting cases; in fact, for distances $\mathbf{r}$ such that $\lambda \gg |\mathbf{r}| \gg a$ it may still be meaningful to define a local strain, and

$$\langle [e(\mathbf{r}^i|p) - e(\mathbf{r}^i + \mathbf{r}|p)]^2 \rangle \propto \omega_p^{-2\bar{d}/D} \tag{8}$$

may be a good approximation. However, if we take this average for nearest neighbors ($|\mathbf{r}| = a$) we must obtain an ω_p^2 dependence due to energy equipartition, since the left-hand side of (8) in this case is proportional to the potential energy of mode p.[22] Therefore, we are faced with two different ω behaviors, and one should be careful in using scaling arguments. For example, for processes that depend mainly on the displacement difference between neighboring masses, an ω^2 scaling might be the most suitable; this could be the case of one-fracton-induced relaxation in paramagnetic ions, where it is local modulations of the crystal field that cause the process. On the other hand, for one-fracton-induced energy transfer between "distant" ions the other scaling law might be more appropriate. As we shall see in the following, in the case of Raman scattering neither law works.

We believe that scaling arguments involving average properties characterized by parameters such as $\bar{d}$, D, and d_ϕ (or σ) cannot describe physical properties, which depend on local dynamical conditions in the presence of important fluctuations.

IV. DYNAMICAL STRUCTURE FACTOR

The square of the Fourier transform $f(\mathbf{k}, p)$ is related to the dynamical structure factor:

$$S(\mathbf{k}, \omega) \propto \frac{n(\omega)+1}{\omega} \sum_p \delta(\omega - \omega_p) |f(\mathbf{k}, p)|^2, \tag{9}$$

which in turn determines the shape of one-fracton scattering spectra such as Brillouin and coherent neutron scattering. In Fig. 5 we report $|f(\mathbf{k}, p)|^2$ for some k values along the x direction and for different concentrations. The phonon or fracton nature of the modes is reflected in the width of the features. At percolation threshold a large distribution of fractons contributes at each reported k value, while at higher concentrations the sharp, low-k patterns indicate the phonon character of the involved modes. In the phonon regime the ω of the peaks, ω_m, are proportional to k, as they should be, yielding the sound velocity as a function of concentration, while in the fracton regime they obey the scaling relation seen in the preceding section. Note that at percolation threshold [Fig. 5(c)] the features have the same form as required by statistical self-similarity, so that both ω_m and the whole shape scales as $k^{\bar{d}/D}$. Thanks to this property, the shapes in Fig. 5(c) also reproduce the Brillouin spectra of fractals, even though in actual experiments the involved k values are about two orders of magnitude smaller than what can be achieved in our limited lattices. The Brillouin spectrum is actually given by Eq. (9), which for $\hbar\omega \ll k_B T$ means multiplying the shapes of Fig. 5 by $1/\omega^2$; this does not significantly affect the sharp phonon peaks, but completely wipes out the maxima of the broad fracton features, and the spectrum results in a continuous descent from the Rayleigh line. From Fig. 5(b) we may

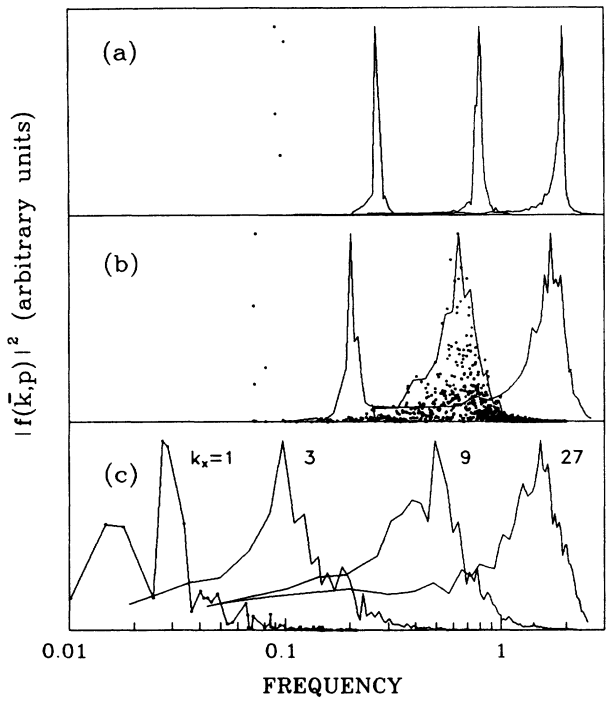

FIG. 5. Squared Fourier transform of the vibrational modes as a function of the mode frequency, for four different k values in the x direction (k=1, 3, 9, 27 in units of $2\pi/L$, where $L = 65a$ is the lattice size). Concentrations are as follows: (a) $c = 0.95$; (b) $c = 0.8$; (c) $c = 0.59$. Apart from (c), k=1, the full lines are obtained by averaging the computed transforms whose actual look is shown in (b), k=9.

presume that for concentrations higher than percolation threshold the spectrum evolves from phononlike to fractonlike by increasing the exchanged k. These predictions are in general agreement with the experimental results of Courtens *et al.* in silica aerogels.[7]

V. THEORY OF RAMAN SCATTERING

In general, the light-scattering spectrum of a system consisting of elementary scatterers characterized by a bare polarizability

$$[\alpha]_{\alpha\beta} = \alpha\delta_{\alpha\beta} + [\beta]_{\alpha\beta}, \tag{10}$$

is given in terms of the scattering coefficients $I_{\alpha\beta\gamma\delta}(\omega,\mathbf{k})$ by

$$I_\Gamma(\omega) = J_0 \rho V \frac{\omega_i \omega_s^3}{c^4} \Delta\Omega \sum_{\alpha\beta\gamma\delta} \hat{n}_\alpha \hat{m}_\beta \hat{n}_\gamma \hat{m}_\delta I_{\alpha\beta\gamma\delta}(\omega,\mathbf{k}), \tag{11}$$

where $\Gamma \equiv (\hat{\mathbf{n}},\hat{\mathbf{m}},\mathbf{k}_i,\mathbf{k}_s)$ represents the scattering configuration as defined by the wave vectors of the incident ($\mathbf{k}_i$) and scattered ($\mathbf{k}_s$) radiation, and $\mathbf{k} = \mathbf{k}_i - \mathbf{k}_s$. In Eq. (11) ω_i and ω_s are the frequency of the incident and scattered radiation, respectively, $\omega = \omega_i - \omega_s$, ρ is the number density, V is the scattering volume, J_0 the incident photons flux, and $\Delta\Omega$ the accepted solid angle. The scattering coefficients are defined as

$$I_{\alpha\beta\gamma\delta}(\omega,\mathbf{k}) = \frac{1}{2\pi N}\int dt e^{i\omega t} \sum_{ij} \langle e^{-i\mathbf{k}\cdot[\mathbf{R}^i(t)-\mathbf{R}^j(0)]} \pi^i_{\alpha\beta}(t)\pi^j_{\gamma\delta}(0)\rangle. \tag{12}$$

Here $\pi^i_{\alpha\beta}(t)$ is the instantaneous effective polarizability of the ith scatterer whose instantaneous position is $\mathbf{R}^i(t) = \mathbf{r}^i + \mathbf{u}^i(t)$. In an isotropic system it is enough to know the $I_{\alpha\beta\alpha\beta}(\omega,\mathbf{q})$ coefficients for $\alpha = \beta$ (polarized scattering) and $\alpha \neq \beta$ (depolarized scattering).

Equation (12) accounts for both Brillouin and Raman scattering. Roughly speaking, the former originates from the exponential factor and the latter from the polarizability factor; as we have seen in the preceding section (Fig. 5), in our systems there is a contribution of the exponential factor at all frequencies which in principle interferes with the Raman contribution. However, due to the smallness of the light wave vector, it is reasonable to neglect such effect and just take $\mathcal{K} = 0$ in Eq. (12):

$$I_{\alpha\beta}(\omega) \equiv I_{\alpha\beta\gamma\delta}(\omega,\mathcal{K}=0) = \frac{1}{2\pi N}\int dt e^{i\omega t} \sum_{ij} \langle \pi^i_{\alpha\beta}(t)\pi^j_{\alpha\beta}(0)\rangle. \tag{13}$$

Let us expand the polarizability in power series of the displacements around the equilibrium positions of the scatterers

$$\pi^i_{\alpha\beta}(t) = \pi^i_{\alpha\beta} + \sum_{j,\gamma} \frac{\partial \pi^i_{\alpha\beta}}{\partial u^j_\gamma} u^j_\gamma(t), \tag{14}$$

where the quantities $\pi^i_{\alpha\beta}$ and $\partial\pi^i_{\alpha\beta}/\partial u^j_\gamma$ are evaluated at equilibrium configuration. With the use of Eqs. (1) and (14), and neglecting the elastic contribution, Eq. (12) becomes

$$I_{\alpha\beta}(\omega) = \frac{1}{2\pi N}\frac{\hbar}{2NM}\sum_{pp'}\frac{1}{\sqrt{\omega_p\omega_{p'}}}\sum_{ij}\sum_{i'j'}\sum_{\gamma\gamma'} e_\gamma(j|p)e_{\gamma'}(j'|p')\frac{\partial\pi^i_{\alpha\beta}}{\partial u^j_\gamma}\frac{\partial\pi^{i'}_{\alpha\beta}}{\partial u^{j'}_{\gamma'}}\int dt e^{i\omega t}\langle A_p(t)A_{p'}(0)\rangle. \tag{15}$$

Using

$$\frac{1}{2\pi}\int dt e^{i\omega t}\langle A_p(t)A_{p'}(0)\rangle = \delta_{pp'}\{[n(\omega_p)+1]\delta(\omega-\omega_p) + n(\omega_p)\delta(\omega+\omega_p)\}, \tag{16}$$

we obtain for the Stokes part of the spectrum

$$I_{\alpha\beta}(\omega)=\frac{\hbar}{2N^2M}\sum_p\frac{n(\omega_p)+1}{\omega_p}\delta(\omega-\omega_p)\left|\sum_{ij}\sum_\gamma\frac{\partial\pi^i_{\alpha\beta}}{\partial u^j_\gamma}e_\gamma(j|p)\right|^2. \tag{17}$$

If we define $C_{\alpha\beta}(p)$ as

$$C_{\alpha\beta}(p)=\frac{1}{N^2}\left|\sum_{ij}\sum_\gamma\frac{\partial\pi^i_{\alpha\beta}}{\partial u^j_\gamma}e_\gamma(j|p)\right|^2 \tag{18}$$

and $\mathcal{C}_{\alpha\beta}(\omega)$ as

$$\mathcal{C}_{\alpha\beta}(\omega)=\frac{\sum_p C_{\alpha\beta}(p)\delta(\omega-\omega_p)}{\sum_p\delta(\omega-\omega_p)}, \tag{19}$$

we obtain the well-known expression for the scattered intensity,

$$I_{\alpha\beta}(\omega)=\frac{\hbar}{2M}\frac{n(\omega)+1}{\omega}\rho(\omega)\mathcal{C}_{\alpha\beta}(\omega). \tag{20}$$

Expression (18) determines the coupling coefficient as a function of the variation of the effective polarizability tensor of the ith scatterer induced by a unitary displacement of the jth mass, and of the eigenvector of the pth mode.

We will now discuss the ω dependence of $\mathcal{C}(\omega)$ proposed so far in the literature, and the hypotheses under which these dependences can be obtained by Eqs. (18) and (19).

In order to establish a comparison with previous works, we note that since a rigid displacement of the whole system does not affect the polarizability, we have

$$\sum_j\frac{\partial\pi^i_{\alpha\beta}}{\partial u^j_\gamma}=0 \tag{21}$$

so that (18) can be rewritten as

$$C_{\alpha\beta}(p)=\frac{1}{N^2}\left|\sum_{ij}\sum_\gamma\frac{\partial\pi^i_{\alpha\beta}}{\partial u^j_\gamma}[e_\gamma(j|p)-e_\gamma(i|p)]\right|^2, \tag{22}$$

which shows that the coefficient $C_{\alpha\beta}(p)$, which measures the coupling of the radiation with the pth normal mode of the system, depends on the relative shift of scatterers i and j when subject to that mode, weighed by the function $\partial\pi^i_{\alpha\beta}/\partial u^j_\gamma$, which depends on the equilibrium position of particles i and j. In an ordered system the quantities $\partial\pi^i_{\alpha\beta}/\partial u^j_\gamma$ depend only on the relative distance between particles i and j, but this is not true in a disordered system.

The ω dependence of $\mathcal{C}_{\alpha\beta}(\omega)$ found in Refs. 2 and 3 can be obtained from the general form (22) as follows.

(i) Polarizability modulation takes place only among nearest neighbors, i.e., say only $j=i+1$ contributes to the sum in Eq. (22).

(ii) The quantities $V^i_{\alpha\beta\gamma}=\partial\pi^i_{\alpha\beta}/\partial u^{i+1}_\gamma$ can be formally split into a spatial mean part $\langle V_{\alpha\beta\gamma}\rangle=1/N\sum_i V^i_{\alpha\beta\gamma}$ and a fluctuating part $\delta V^i_{\alpha\beta\gamma}=V^i_{\alpha\beta\gamma}-\langle V_{\alpha\beta\gamma}\rangle$. As can easily be seen, because of the conservation of the center of mass of the entire system [see Eq. (2)], the mean part $\langle V_{\alpha\beta\gamma}\rangle$ does not contribute to the Raman scattering.

(iii) An ensemble average of Eq. (22) (hereafter indicated with an overline) is introduced in order to handle the fluctuating quantities $\delta V^i_{\alpha\beta\gamma}$.

(iv) Following Jackle[23] one neglects any correlation between the polarizability derivative and the eigenvectors (i.e., independent mechanical and electrical disorders) and assumes that the polarizability fluctuations in different sites are uncorrelated:

$$\overline{\delta V^i_{\alpha\beta\gamma}\delta V^j_{\alpha\beta\gamma}}=\delta_{ij}|\delta V_{\alpha\beta\gamma}|^2. \tag{23}$$

With the preceding assumption the expression for the configurationally averaged $C_{\alpha\beta}(p)$ becomes

$$\overline{C_{\alpha\beta}(p)}=\frac{1}{N^2}\sum_\gamma|\delta V_{\alpha\beta\gamma}|^2\sum_i|e_\gamma(i+1|p)-e_\gamma(i|p)|^2$$
$$\propto\frac{a^2}{N^2}\sum_\gamma|\delta V_{\alpha\beta\gamma}|^2\sum_i|\epsilon_{x\gamma}(\mathbf{r}^i|p)|^2. \tag{24}$$

The average squared strain is then evaluated by scaling arguments from Eq. (8), thus obtaining

$$\frac{1}{N}\sum_i|\epsilon_{\alpha\beta}(\mathbf{r}^i|p)|^2\propto l_p^{-2d_\phi} \tag{25}$$

so that

$$\overline{\mathcal{C}_{\alpha\beta}(\omega)}\propto\omega_p^{\frac{2\bar{d}d_\phi}{D}}. \tag{26}$$

In their derivation of the ω dependence of $\mathcal{C}_{\alpha\beta}(\omega)$ Tsujimi *et al.*[5] followed the procedure of Boukenter *et al.*[2] up to Eq. (24). They also used the scaling law (8) for the strain, but they assumed that the scattering amplitudes from all the l_p^D scatterers involved in mode p add up with constructive interference, i.e., they rewrote Eq. (24) as

$$\overline{\mathcal{C}_{\alpha\beta}(\omega)}\propto\omega_p^{\frac{2\bar{d}d_\phi}{D}-\bar{d}}. \tag{27}$$

We cannot find any justification for such assumption. This term, which is certainly present, adds coherently, and its only effect is to renormalize the Brillouin intensity because it represents the contribution to the polarizability modulation of a given atom produced by atoms placed at a distance comparable with the wavelength of the radiation; it does not contain any fluctuating component and does not produce disorder-induced Raman scattering. The main contribution to the scattering comes from the fluctuations of polarizability related to the mi-

croscopic disorder of the structure (i.e., electrical disorder) and to the way such fluctuations are correlated to the local displacement fluctuations due to the pth mode (mechanical disorder).

In our calculation we will use as a starting point Eq. (18) without introducing any further assumption. We will consider masses with identical bare spherical polarizability, α, thereby neglecting the cases in which scattering originates from the anisotropic part of the polarizability (β) modulated by the normal modes through rotational-translational coupling. The effective polarizability $\pi^i_{\alpha\beta}(t)$ will therefore be written[24]

$$\pi^i_{\alpha\beta}(t) = \alpha\delta_{\alpha\beta} + \Delta\pi^i_{\alpha\beta}(\{\mathbf{R}^j(t)\}_{j=1,\ldots,N}), \tag{28}$$

where the second (induced) term depends, in principle, on the position of all masses of the system and is the main source of Raman scattering in solid systems. To go further, one must know the function $\Delta\pi^i_{\alpha\beta}(\{\mathbf{R}^j(t)\}_{j=1,\ldots,N})$ explicitly. There are two limiting cases where this is possible.

A. Bond polarizability (BP)

In this model one assumes that the incremental polarizability tensor depends only on the relative distance of nearest-neighbor atoms, that it is pairwise additive, and that it has cylindrical symmetry around the vector $\mathbf{R}^{ij}(t) = \mathbf{R}^i(t) - \mathbf{R}^j(t)$, i.e.,

$$^{\mathrm{BP}}\Delta\pi^i_{\alpha\beta}(t) = \sum_{j\in \mathrm{NN}(i)} [\hat{\mathbf{T}}^{(2)}_{\alpha\beta}(\hat{\mathbf{R}}^{ij}(t))h(|\mathbf{R}^{ij}(t)|) + g(|\mathbf{R}^{ij}(t)|)\delta_{\alpha\beta}], \tag{29}$$

where $\hat{\mathbf{T}}^{(2)}_{\alpha\beta}(\hat{\mathbf{R}}) = 3\hat{\mathbf{R}}_\alpha\hat{\mathbf{R}}_\beta - \delta_{\alpha\beta}$, NN($i$) indicate the set of atoms which are nearest neighbors of the atom i and the functions $g(|\mathbf{R}|)$ and $h(|\mathbf{R}|)$ determine the dependence of the isotropic and anisotropic parts of the induced polarizability, respectively, on the instantaneous distance between nearest neighbors. This model is generally employed in describing the Raman scattering in covalent solids.

B. Dipole induced dipole (DID)

Strictly speaking the DID is not a model but rather describes phenomena that are always present in condensed matter. Indeed it is DID that is responsible for the renormalization of the bare polarizability, which yields the Lorentz-Lorenz relation. Moreover it has been recognized as the major source of Raman scattering in dense systems.

The derivation of $^{\mathrm{DID}}\Delta\pi^i_{\alpha\beta}(t)$ is straightforward, and we will briefly describe it. Let $\tilde{\mu}^i_\alpha = \alpha(\mathcal{E}_\alpha + E^i_\alpha)$ be the α component of the effective dipole moment of the ith mass in the presence of the electric field $\boldsymbol{\mathcal{E}}$ of the incident laser beam and of the electric field

$$E^i_\alpha = \sum_j \sum_\beta \hat{\mathbf{T}}^{(2)}_{\alpha\beta}(\hat{\mathbf{R}}^{ij}(t))\frac{1}{|\mathbf{R}^{ij}(t)|^3}\tilde{\mu}^j_\beta, \tag{30}$$

which is the sum of the fields produced by all other effective dipoles, so that

$$\tilde{\mu}^i_\alpha(t) = \alpha\left(\mathcal{E}_\alpha + \sum_j \sum_\beta \hat{\mathbf{T}}^{(2)}_{\alpha\beta}(\hat{\mathbf{R}}^{ij}(t))\frac{1}{|\mathbf{R}^{ij}(t)|^3}\tilde{\mu}^j_\beta(t)\right). \tag{31}$$

The self-consistent relationship for the effective polarizability is obtained from its definition

$$\pi^i_{\alpha\beta}(t) = \left(\frac{\partial\tilde{\mu}^i_\alpha(t)}{\partial\mathcal{E}_\beta}\right)_{\boldsymbol{\mathcal{E}}=0} \tag{32}$$

to be

$$\pi^i_{\alpha\beta}(t) = \alpha\delta_{\alpha\beta} + \alpha\sum_\gamma \sum_j \hat{\mathbf{T}}^{(2)}_{\alpha\gamma}(\hat{\mathbf{R}}^{ij}(t))\frac{1}{|\mathbf{R}^{ij}(t)|^3}\pi^j_{\gamma\beta}(t). \tag{33}$$

At first order (i.e., by taking $\pi^j_{\gamma\beta} = \alpha\delta_{\gamma\beta}$ on the right-hand side), we obtain the closed form

$$\pi^i_{\alpha\beta}(t) = \alpha\delta_{\alpha\beta} + \alpha^2\sum_j \hat{\mathbf{T}}^{(2)}_{\alpha\beta}(\hat{\mathbf{R}}^{ij}(t))\frac{1}{|\mathbf{R}^{ij}(t)|^3} \tag{34}$$

and finally

$$^{\mathrm{DID}}\Delta\pi^i_{\alpha\beta}(t) = \alpha^2\sum_j \hat{\mathbf{T}}^{(2)}_{\alpha\beta}(\hat{\mathbf{R}}^{ij}(t))\frac{1}{|\mathbf{R}^{ij}(t)|^3}. \tag{35}$$

By differentiating Eq. (34) and calculating the result at equilibrium we also obtain

$$^{\mathrm{DID}}\left(\frac{\partial\pi^i_{\alpha\beta}}{\partial u^j_\gamma}\right) = \frac{2\alpha^2}{a^4}\hat{\mathbf{T}}^{(3)}_{\alpha\beta\gamma}(\hat{\mathbf{r}}^{ij}), \tag{36}$$

where

$$\hat{\mathbf{T}}^{(3)}_{\alpha\beta\gamma}(\hat{\mathbf{R}}) = 15\hat{\mathbf{R}}_\alpha\hat{\mathbf{R}}_\beta\hat{\mathbf{R}}_\gamma - 3(\delta_{\alpha\beta}\hat{\mathbf{R}}_\gamma + \delta_{\gamma\beta}\hat{\mathbf{R}}_\alpha + \delta_{\alpha\gamma}\hat{\mathbf{R}}_\beta). \tag{37}$$

Note that if one considers the DID expression for $\Delta\pi^i_{\alpha\beta}$, and limits the sum in Eq. (35) to nearest neighbors alone, one formally turns to the BP model if in the latter we put $h(R) = \alpha^2/R^3$ and $g(R) = 0$. In our numerical calculation we have computed Eq. (35) both by summing the contributions of all masses (full DID), and in the limiting case of interaction to nearest neighbors alone (NN DID) in order to simulate the BP model.

VI. NUMERICAL RESULTS

In Fig. 6 we report in log-log scale the DID and BP computed Raman scattering coefficients $C_{xx}(\omega)$ for three-dimensional lattices of linear dimensions 29, 19, and 15 at concentrations of 0.312, 0.5, and 0.6, respectively. In order to reduce statistical fluctuations, at percola-

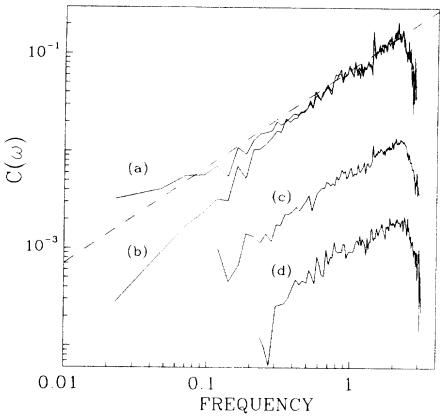

FIG. 6. Polarized Raman coupling coefficient $\mathcal{C}_{xx}(\omega)$ for three-dimensional lattices. (a) full DID averaged over three 29×29×29 clusters, $c = 0.312$; (b) as (a) but NN DID; (c) full DID averaged over three 19×19×19 clusters, $c = 0.5$; (d) full DID of one 15×15×15 cluster, $c = 0.7$. All traces give absolute Raman coupling coefficient normalized to the number of masses in the cluster assuming isotropic polarizability $\alpha = 1$. Trace (d) is shifted down by a decade. A dashed line of slope 1 is reported as a guide to the eye.

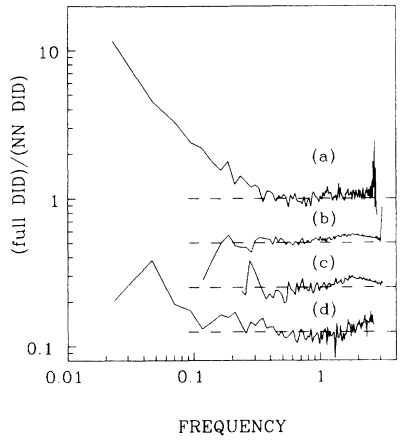

FIG. 7. Ratio of full DID to NN DID in a log-log scale. (a) 29×29×29, $c = 0.312$; (b) 19×19×19, $c = 0.5$; (c) 15x15x15, $c = 0.7$; (d) 65x65, $c = 0.59$. Traces (b), (c), and (d) have been shifted down by factors 2, 4, and 8, respectively; the dashed lines indicate the respective unit ratios.

tion threshold we averaged over different realizations of our sample and over all the modes having their eigenfrequency within a $\Delta\omega = 0.022$ interval around any frequency value reported. In fact, the computed $\mathcal{C}_{xx}(\omega)$ is an extremely fluctuating function of the mode; most modes give a negligible contribution, so that it is necessary to average over a large number in order to obtain a reasonably smooth function. At percolation threshold [Fig. 6(a)] and in the range $\omega \gtrsim 0.2$, DID gives $\mathcal{C}_{xx}(\omega) \tilde{\propto} \omega$ and BP [Fig. 7(b)] parallels it; at lower frequencies, where the DID result becomes less frequency dependent, the two curves become appreciably different. It seems that for neither mechanism does a single slope exist in the whole calculated frequency range.

The different behaviors of DID and BP, whose ratio is shown for the three concentrations in Fig. 7, can be understood as follows. In the BP case the modulation of polarizability takes place only if nearest neighbors are connected, so that there exists a close phase relationship between their displacements caused by a normal mode. On the other hand, the DID effect has a purely electromagnetic nature; this implies that there is polarizability modulation between masses, which are not directly dynamically connected, but which, due to the fractal structure, may be rather close in space. For the displacements of these masses under the action of mode p, there will be, in general, no such close phase relationship as exists for connected nearest neighbors. This is evident from a visual inspection of Fig. 2, where there are pairs of spatially close masses on opposite sides of fjords with very different phases. The effect is not very important for high-frequency modes with short λ [see Figs. 1(a) and 1(b)], because phase shifts are also big for dynamically connected neighboring masses, but becomes important at lower frequencies, and this produces the observed difference between DID and BP results.

When concentration is increased, Figs. 6(c) and 6(d), the Raman coupling coefficient is strongly reduced because disorder is decreased. However, apart from this intensity change, in the high-energy region above the phonon-fracton crossover the DID result for $\mathcal{C}_{xx}(\omega)$ does not appreciably differ from what is obtained at percolation concentration. At low frequency, where the phononlike behavior $\mathcal{C}_{xx}(\omega) \propto \omega^2$ is expected, the slope does increase, but a clearcut fracton-phonon crossover does not seem to be present, even though statistical noise does not allow a definite conclusion to be drawn. As regards the comparison between DID and BP, Fig. 7 shows that by increasing concentration the two results tends to converge. This can be understood by considering that there are fewer spatially neighboring pairs joined by long connected paths in the fractal because the system is more compact.

In Fig. 8 we report the computed depolarization ratios $\mathcal{R}(\omega) = \mathcal{C}_{xy}(\omega)/\mathcal{C}_{xx}(\omega)$, for the three-dimensional lattices; at high frequency all samples approach the 1/3 value, which is predicted for the NN DID (or BP) independent of the mode pattern as it results from Eqs. (36) and (37); at low frequencies, and especially for the percolating cluster, $\mathcal{R}(\omega)$ increases. This is due to the increasing contribution of non-nearest-neighbor pairs, which also produce the low-frequency gap between DID and BP discussed above [Fig. 6(a) and 6(b)].

$\mathcal{C}_{xx}(\omega)$ calculated in two dimensions for different concentrations is shown in Fig. 9 in a log-log scale. At percolation threshold, the slope is about 1 over a wide range of frequencies. At higher concentrations, as in the three-dimensional case, a higher slope is observed in the low-frequency range, but again no sharp fracton-phonon crossover is evident. The phononlike ω^2 dependence is

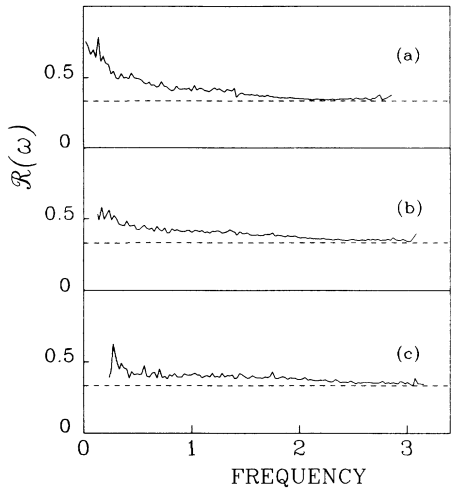

FIG. 8. Depolarization ratio $\mathcal{R}(\omega) = \mathcal{C}_{xy}(\omega)/\mathcal{C}_{xx}(\omega)$ for the three-dimensional lattices of Fig. 6. (a) 29×29×29, c = 0.312; (b) 19x19x19, c = 0.5; (c) 15x15x15, c = 0.7. The dashed lines at $\mathcal{R}(\omega) = 1/3$ correspond to the theoretical prediction for NN DID.

reproduced in the low-energy region of Fig. 9(a), corresponding to the computed Raman coupling coefficient for a perfect lattice with three vacancies included in order to make Raman scattering allowed.

The difference between BP and DID results is much less important in two dimensions than in three. $C_{xx}^{\mathrm{DID}}(\omega)$ is appreciably greater than $C_{xx}^{\mathrm{BP}}(\omega)$ only at percolation threshold and in the lowest-energy region [Fig. 7(d)]. However, the slope of $C_{xx}^{\mathrm{BP}}(\omega)$ still remains ≈ 1 in the whole range. It seems that the effect of non-NN pairs across fjords plays a minor role in two dimensions because in this case there are fewer topological possibilities of realizing such pairs. The effect could possibly become more important at lower frequencies, which are not reachable for us due to computational limits.

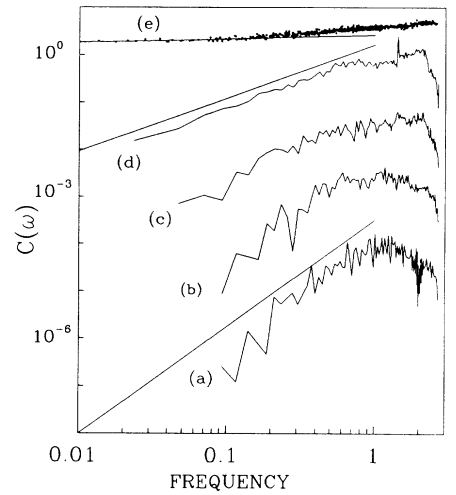

FIG. 9. Polarized Raman coupling coefficient $\mathcal{C}_{xx}(\omega)$ for two-dimensional 65×65 lattices, full DID. (a) perfect lattice with three vacancies; (b) c = 0.9; (c) c = 0.7; (d) c = 0.59, averaged over eight clusters. All traces give absolute Raman coupling coefficient normalized to the number of masses in the cluster assuming isotropic polarizability $\alpha = 1$. Trace (b) is shifted down by a factor of 5. Straight lines of slopes 1 and 2 are reported as guides to the eye. (e) $\mathcal{C}_{xx}(\omega)$ calculated in the approximation of independent fluctuations from different k components (see text); the slope of the superimposed straight line is $0.07 = 2\bar{d}/D - \bar{d}$.

In all of our calculations, the Raman coefficient is observed to drop as the Debye frequency is approached. This is not connected to the similar behavior of the density of states; the decrease in $\mathcal{C}_{xx}(\omega)$ is a general property of disordered systems and will be the subject of a detailed further study.[25]

A relevant question is whether the finite size of our lattices, together with cyclic boundary conditions, might prejudice our low-frequency results. Actually, visual inspection of several modes of the 65×65 percolating lattice shows that fractons are well localized only for $\omega \geq 0.3$; however, from Fig. 4 we see that the scaling relationship $\omega \propto k^{\bar{d}/D}$, which is typical of fractons, holds also at lower frequencies, indicating that cyclic conditions, which affect the localization length, are ineffective on the short-range fluctuations, which produce Raman scattering. We have verified that in passing from 20×20 to 100×100 (single diagonalization) lattices no relevant slope change in $\mathcal{C}_{xx}(\omega)$ occurs within the statistical noise.

VII. DISCUSSION

Our numerical results indicate that the scaling laws proposed so far (see Sec. V) do not work; in fact we have shown that in three dimensions the BP and DID calculations yield different results for the coupling coefficient and that a single slope is not appropriate for either mechanism in the whole energy range (Figs. 6 and 7). Let us consider the simplest possible case, i.e., NN DID (or BP), where the coupling coefficient for polarized Raman scattering relative to the pth mode is given by

$$C_{xx}^{\mathrm{BP}}(p) \propto \left| \sum_{i}{}' [e(i+1|p) - e(i|p)] \right|^2 . \tag{38}$$

Here the prime indicates that the summation is limited to the masses, which have a neighboring mass in the positive x direction.

Equation (38) was used to produce Fig. 6(b), where a slope continuously changing from about 1.4 to about 1.1 is observed in three-dimensional lattices. In two dimensions Eq. (38) gives a nearly linear dependence on a long-frequency range very much like Fig. 9(d) (full DID). This equation looks simple, and it would seem surprising that a simple scaling law for it is not found. However, its simpleness is only apparent: Eq. (38) exhibits the space-fluctuation origin of the Raman scattering.

This point deserves to be stressed: We will show that only in particular cases can a scaling law for a fluctuating quantity, such as Eq. (38), be obtained in terms of average quantities. If we insert the inverse Fourier transform

of Eq. (6) into Eq. (38) we obtain

$$C_{xx}^{\mathrm{BP}}(p) \propto \left| \sum_{\mathbf{k}} f(\mathbf{k},p) \sum_{i}{}' e^{i\mathbf{k}\cdot\mathbf{r}_i}(e^{ik_x a}-1) \right|^2 . \quad (39)$$

This expression gives a simple result if the pth mode is phononlike with a well-defined $\mathbf{k}$ vector $\mathcal{K}_p$, i.e., when the function $f(\mathbf{k},p)$ is sharply peaked around $\mathcal{K}_p$. A single term in the summation over $\mathbf{k}$ contributes appreciably, and in the low-frequency limit ($|\mathbf{k}|a << 1$) we get

$$C_{xx}^{\mathrm{BP}}(p) \propto |\mathcal{K}_p|^2 \left| \sum_{i}{}' e^{i\mathcal{K}_p\cdot\mathbf{r}_i} \right|^2 . \quad (40)$$

As mentioned, this would be zero for a perfect crystal, i.e.,

$$\left| \sum_{i}{}' e^{i\mathbf{k}\cdot\mathbf{r}_i} \right|^2 = \left| \sum_{i} e^{i\mathbf{k}\cdot\mathbf{r}_i} - \sum_{i}{}'' e^{i\mathbf{k}\cdot\mathbf{r}_i} \right|^2 = \left| \sum_{i}{}'' e^{i\mathbf{k}\cdot\mathbf{r}_i} \right|^2 , \quad (41)$$

where the double primed sum is on the missing bonds and measures the structure factor of disorder.

For a homogeneous distribution of defects the latter quantity is constant on average: No k dependence is expected, though it is not a smooth quantity because of its intrinsic fluctuating nature. Therefore, for phonons in a disordered system we obtain $C_{xx}^{\mathrm{BP}}(p) \propto |\mathcal{K}_p|^2$, i.e., $\mathcal{C}_{xx}^{\mathrm{BP}}(\omega) \propto \omega_p^2$ as an average over many nearly degenerate modes. The same result is obtained in real space from Eq. (38) by assuming that the fluctuations of the relative displacements (i.e., of local strain) are proportional to the quantity itself, and that the scattering contributions add incoherently. In any case, one assumes that the modes are well characterized by a single-k component, so that both the local strain and its fluctuations are proportional to k.

The impossibility of extending such an argument to fractons is evident also from the mentioned difficulty of defining an average local strain [see Fig. 2(b)]. In any case, both scaling laws[2,22] overestimate the slope in two dimensions; the hypothesis that the fluctuations are proportional to the quantity and that scattering contributions add incoherently fails. It may be interesting to study the problem in the Fourier space starting from Eq. (39). For phonons in a disordered structure, but in particular for fractons, $f(\mathbf{k},p)$ is extended over large intervals of $\mathbf{k}$ space, as has been shown in Fig. 3, and Eq. (39) becomes intractable. However, let us see what happens if one wrongly treats the fluctuations in bond lengths due to different k components as independent, obtaining

$$C_{xx}^{\mathrm{BP}}(p) \propto \sum_{\mathbf{k}} |f(\mathbf{k},p)|^2 |(e^{ik_x a}-1)|^2 \cdot \left| \sum_{i}{}' e^{i\mathbf{k}\cdot\mathbf{r}_i} \right|^2 . \quad (42)$$

This quantity, which was computed for each mode of a 65×65 square lattice at percolation threshold, is reported in Fig. 9(e) and has a smooth flat dependence on frequency. It is also possible to find an analytical form for this quantity, by using scaling arguments. By taking for the structure factor of bonds the same scaling law as for the structure factor of masses, $S(\mathbf{k})$,

$$\left| \sum_{i}{}' e^{i\mathbf{k}\cdot\mathbf{r}_i} \right|^2 \propto \left| \sum_{i} e^{i\mathbf{k}\cdot\mathbf{r}_i} \right|^2 \propto S(\mathbf{k}) \propto k^{-D} \quad (43)$$

and assuming that dynamical structure factor $S(\mathbf{k},\omega_p) \propto |f(\mathbf{k},p)|^2$ scales as a whole as does its maximum (Fig. 5), we obtain for $ka << 1$

$$C_{xx}^{\mathrm{BP}}(p) \propto \sum_{\mathbf{k}} S(\mathbf{k},\omega_p) S(\mathbf{k}) k^2 \propto \mathcal{K}_p^{-D} \mathcal{K}_p^2 \quad (44)$$

or

$$\mathcal{C}_{xx}^{\mathrm{BP}}(\omega) \propto \omega^{2\bar{d}/D-\bar{d}} . \quad (45)$$

Taking $\bar{d} = 4/3$ and $D = 1.89$ we have an $\omega^{0.07}$ dependence, i.e. the straight line in Fig. 9(e), which fits well the low energy part of Eq. (42). The same results would be evidently obtained by assuming a single k component for the fracton and again the scaling relation $\omega \propto k^{\bar{d}/D}$. The scaling law (45), apart from the absence of d_ϕ (or σ) factor, is the same as proposed by Tsujimi *et al.*[5] and Alexander.[21] It is not a good approximation for the evaluation of Eq. (38), which actually yields a slope of about 1 in the two-dimensional lattice.

For the calculation of Raman scattering it is not appropriate to consider the different k components of the relative displacements as independent, or to consider a single effective k value. This is why we are not able to produce a scaling relation for $\mathcal{C}(\omega)$ even in its simplest form (38), let alone the case of full DID, where the induced polarization fluctuations are a complicated function of the mutual distances between masses, as discussed in Secs. V and VI.

In conclusion, our arguments indicate that the formulas so far proposed for the Raman coupling coefficient, which were derived from scaling arguments in terms of the macroscopic parameters $\bar{d}$, D, and d_ϕ (or σ) are unreliable. The essential disorder of statistical fractals, where there are defects at all length scales, makes it impossible to sum incoherently effects of fluctuations at different points within the fracton wavelength, as well as to find a scaling relation for the fluctuations in terms of average quantities such as local strain. The microscopic structure of the system and the actual scattering mechanism seem to determine the shape of the scattering spectrum at least to the same extent as do the macroscopic properties described by the fractal parameters.

ACKNOWLEDGMENT

Valuable discussions with R. Orbach are gratefully acknowledged.

[1] S. Alexander, O. Entin-Wohlman, and R. Orbach, Phys. Rev. B **32**, 6447 (1985).
[2] A. Boukenter, B. Champagnon, E. Duval, J. Dumas, J.F. Quinon, and J. Serughetti, Phys. Rev. Lett. **57**, 2391 (1986).
[3] E. Duval, G. Mariotto, M. Montagna, O. Pilla, G. Viliani, and M. Barland, Europhys. Lett. **3**, 33 (1987).
[4] A. Fontana, F. Rocca, and M.P. Fontana, Phys. Rev. Lett. **58**, 503 (1987).
[5] Y. Tsujimi, E. Courtens, J. Pelous, and R. Vacher, Phys. Rev. Lett. **60**, 2757 (1988).
[6] E. Courtens, J. Pelous, J. Phalippou, R. Vacher, and T. Woignier, Phys. Rev. Lett. **58**, 128 (1987).
[7] E. Courtens, R. Vacher, J. Pelous, and T. Woignier, Europhys. Lett. **6**, 245 (1988).
[8] R. Vacher, T. Woignier, J. Pelous, G. Coddens, and E. Courtens, Europhys. Lett. **8**, 161 (1989).
[9] R. Vacher, E. Courtens, G. Coddens, J. Pelous, and T. Woignier, Phys. Rev. B **39**, 7384 (1989).
[10] R. Vacher, E. Courtens, G. Coddens, A. Heidemann, Y. Tsujimi, J. Pelous, and M. Foret, Phys. Rev. Lett. **65**, 1008 (1990).
[11] J.L. Rousset, A. Boukenter, B. Champagnon, J. Dumas, E. Duval, J.F. Quinon, and J. Serughetti, J. Phys. Condens. Matter **2**, 8445 (1990).
[12] M. Montagna, O. Pilla, G. Viliani, V. Mazzacurati, G. Ruocco, and G. Signorelli, Phys. Rev. Lett. **65**, 1136 (1990).
[13] G.S. Grest and I. Webman, J. Phys. (Paris) Lett. **45**, L1155 (1984).
[14] K. Yakubo and T. Nakayama, Phys. Rev. B **36**, 8933 (1987).
[15] K. Yakubo and T. Nakayama, Phys. Rev. B **40**, 517 (1989).
[16] K. Yakubo and T. Nakayama, J. Phys. Soc. Jpn. **58**, 1504 (1989).
[17] T. Nakayama, K. Yakubo, and R. Orbach, J. Phys. Soc. Jpn. **58**, 1891 (1989).
[18] S. Alexander and R. Orbach, J. Phys. (Paris) Lett. **43**, L625 (1982).
[19] R. Rammal and G. Toulouse, J. Phys. (Paris) Lett. **44**, L13 (1983).
[20] M. Montagna, O. Pilla, and G. Viliani, Philos. Mag. B **59**, 49 (1989).
[21] S. Alexander, Phys. Rev. B **40**, 7953 (1989).
[22] T. Keyes and T. Ohtsuki, Phys. Rev. Lett. **59**, 603 (1987).
[23] J. Jackle, *Amorphous Solids: Low Temperatures Properties* (Springer, Berlin, 1981), Chap. 8.
[24] A.B. Buckingham, Trans. Faraday Soc. **52**, 7437 (1956).
[25] P. Benassi, O. Pilla, V. Mazzacurati, M. Montagna, G. Ruocco, and G. Signorelli, Phys. Rev. B **44**, 11 734 (1991).

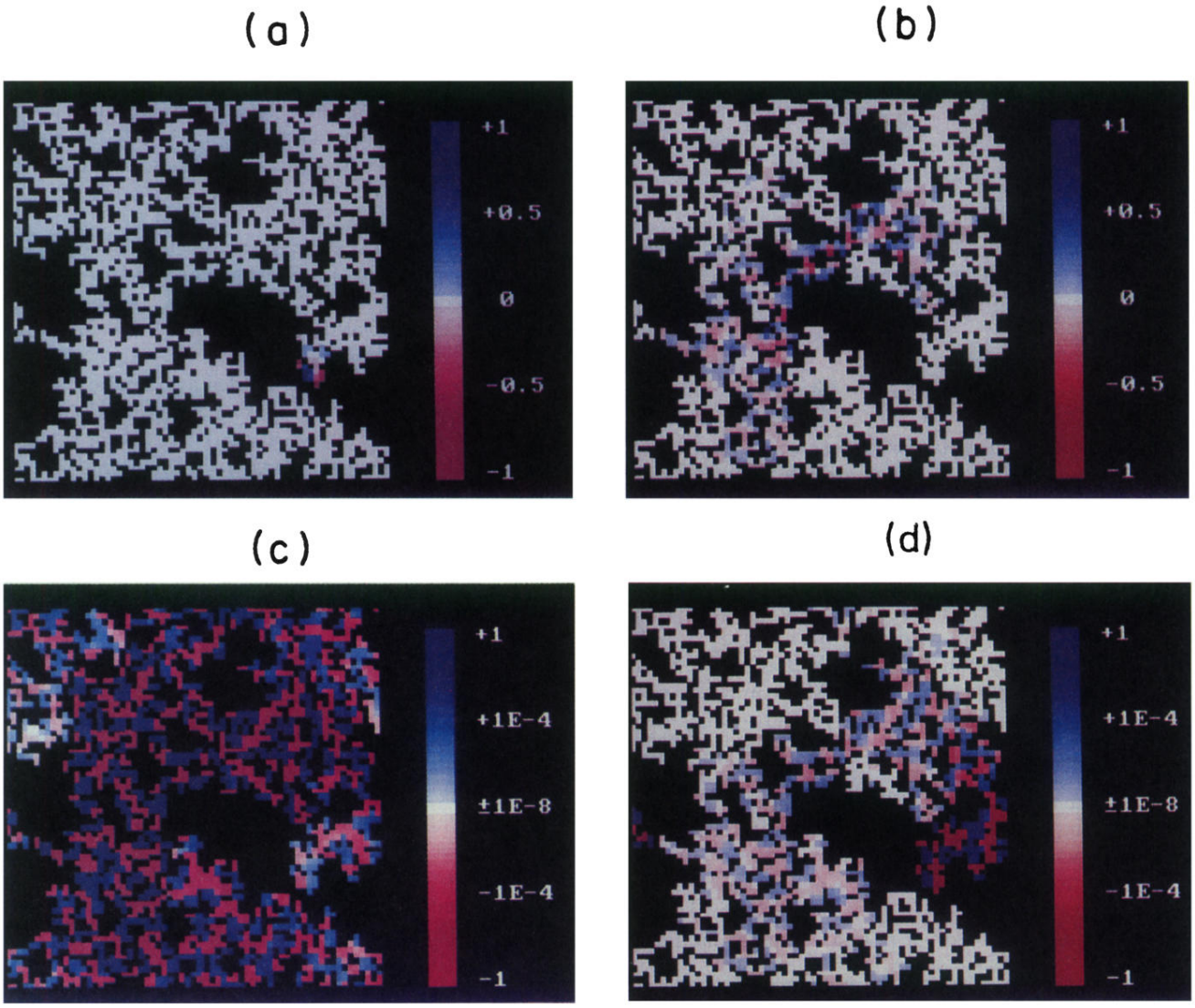

FIG. 1. Vibrational amplitudes of two successive fractons of a 65×65 cluster at percolation threshold. (a) $\omega_1 = 0.802\,04$ (mode A); (b) $\omega_2 = 0.803\,44$ (mode B). (c) and (d), same as (a) and (b) but in a logarithmic scale to enhance the oscillatory behavior of the fracton tails. Frequency in $\sqrt{K/M}$ units: Debye frequency is $2\sqrt{2}$.

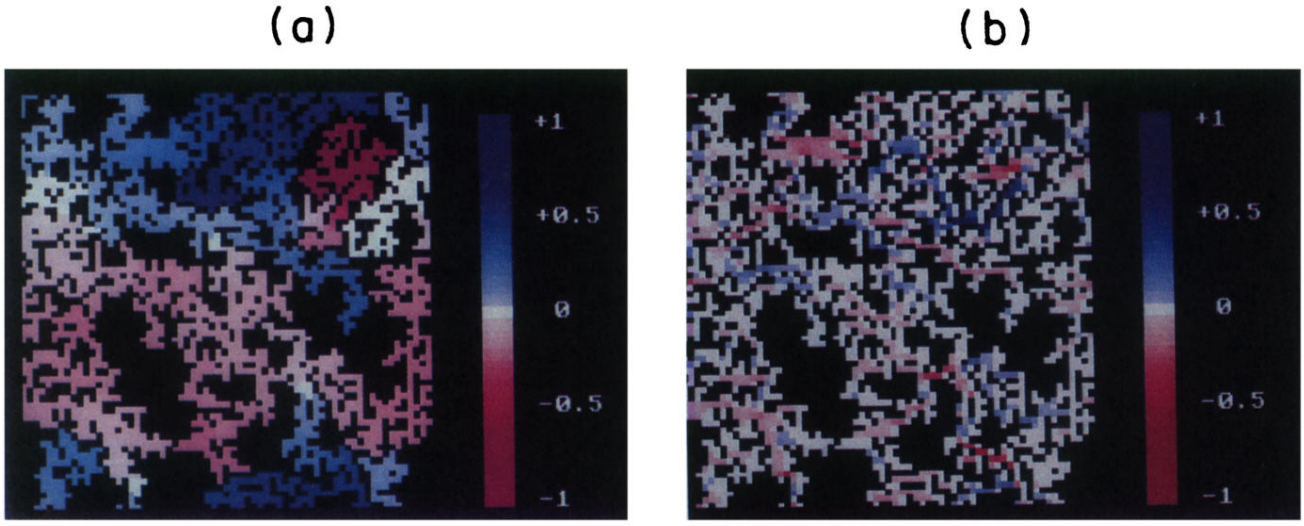

FIG. 2. (a) Vibrational amplitudes of a low-frequency mode ($\omega = 0.022$) of a 65×65 cluster at percolation threshold ($c = 0.59$). (b) displacement difference of any pair of neighboring masses in the x direction (see text).